Harmonic Model Description of the Franck–Condon Density for a Betaine Dye Molecule

ARTICLE *in* THE JOURNAL OF PHYSICAL CHEMISTRY A · MARCH 2004

Impact Factor: 2.69 · DOI: 10.1021/jp0370324

2 AUTHORS, INCLUDING:

Hyonseok Hwang
Kangwon National University
29 PUBLICATIONS **401** CITATIONS

Harmonic Model Description of the Franck−Condon Density for a Betaine Dye Molecule

Hyonseok Hwang and Peter J. Rossky

Institute for Theoretical Chemistry, Department of Chemistry and Biochemistry, University of Texas, Austin, Texas 78712-1167

Received: October 8, 2003; In Final Form: January 27, 2004

Franck−Condon (FC) factors and the FC density associated with an electron transfer reaction are calculated for a betaine molecule, pyridinium-*N*-phenoxide betaine (4-(1-pyridinio)phenolate) in its S_1 excited state. FC factors and density functions for harmonic vibrational modes are computed first by modifying the three level-fixed binary tree algorithm (Ruhoff, P. T.; Ratner, M. A. *Int. J. Quant. Chem.* **2000**, *1*, 383), a sum-over-states method based on recursion relations. This modified method allows the calculation of FC factors for 60 vibrational modes and avoids memory problems due to the large number of modes. The effects on the FC density of frequency shifts and mode mixing (Duschinky rotation) are included. For comparison, the more efficient time-dependent alternative is also employed for the calculation of the FC density function for the harmonic motion. In all cases, for a torsional motion which cannot be described by a harmonic potential, the FC density function is computed through the time-dependent method. We show that the sum-over-states method agrees well with the time-dependent method except for the high-frequency region. There the sum-over-states method is inadequate even when greater than 10^{14} FC factors are included. We find that both frequency shifts and Duschinsky rotation increase the number of FC factors in the high-frequency region, and as a result, they make the FC density function broader. It is shown that frequency shifts have the greater effect. In the high-frequency region we do not observe the strong exponential decay of the FC density function which characterizes the weak coupling limit (relatively small vibrational reorganization energy). We find that the betaine dye falls into the strong coupling limit. The fitting of the FC density function with a simple model which includes one classical degree of freedom and one high-frequency quantal degree of freedom and the comparison of the fitting parameters with comparable exact values show that the simple model provides reasonable physical values such as reorganization energies.

Introduction

Electron-transfer (ET) reactions play an important role in many chemical and biological systems, and there have been many theoretical and experimental studies on ET reaction rates.[1,2] A traditional and conventional approach to ET reaction rate is to neglect the dependence of the electronic coupling matrix element on nuclear displacements (Condon approximation).[3] In that case, the ET reaction rate is factored into the purely electronic part and a purely nuclear part, the so-called Franck−Condon (FC) factors. Because of the importance of the FC factors to ET reaction rates, many theoretical studies have been conducted to calculate the FC factors. Among several methods for the computation of FC factors, one direct approach is a sum-over-states method, which is normally based on recursion relations.[4,5] Alternative time-dependent methods have been introduced by Heller.[6−8] In this method, the FC factors are not calculated directly, but the FC envelop is the Fourier transform of the time-dependent overlap of two nuclear wave functions which are evolving on two different electronic potential energy surfaces (PES).

Sum-over-states methods must be used for the direct calculation of FC factors, but there are some difficulties using that method for large molecules since the equilibrium geometries of two electronic PES are in general rather different. That is, one PES is displaced with respect to the other PES, and frequencies on one PES are shifted from those on the other. Displacements occur from the difference between minima of two PES's, and frequency shifts occur because one PES is distorted from the other. In addition, vibrational normal modes can change so that those in one electronic state are rotated or mixed in the normal-mode basis of the other electronic state. This phenomenon, called a Duschinsky rotation or the Duschinsky effect,[9] prevents FC overlap integrals from being reduced to simple products of one-dimensional FC overlap integrals, and, as a result, the calculation of FC factors becomes more complicated. Because of the significance of FC factors, many methods for computing the integrals along with the Duschinsky rotation have been devised.[10−18] Sharp and Rosenstock have derived expressions based on a generating function method for computing the FC overlap integrals.[10] Gruner and Brumer have used a binary tree algorithm to develop an efficient technique to calculate the vibrational overlap integrals.[11]

As mentioned above, the sum-over-states method is based on recursion relations,[4] and efficient execution of recursion relations requires saving previous overlap integrals in computer memory. However, those methods are challenging to apply directly to large molecules since too many FC overlap integrals must be saved in memory. To address this overflow problem, Ruhoff and Ratner proposed a three level-fixed binary tree (TLFBT) algorithm.[17] This algorithm, discussed below, is based on the Gruner and Brumer's binary tree algorithm,[11] but instead of building one large binary tree, binary trees for each level are constructed to reduce memory usage.

Among studied ET reactions is intramolecular ET, where the ET occurs within a single molecule. A good example of

10.1021/jp0370324 CCC: $27.50
Published on Web 03/11/2004

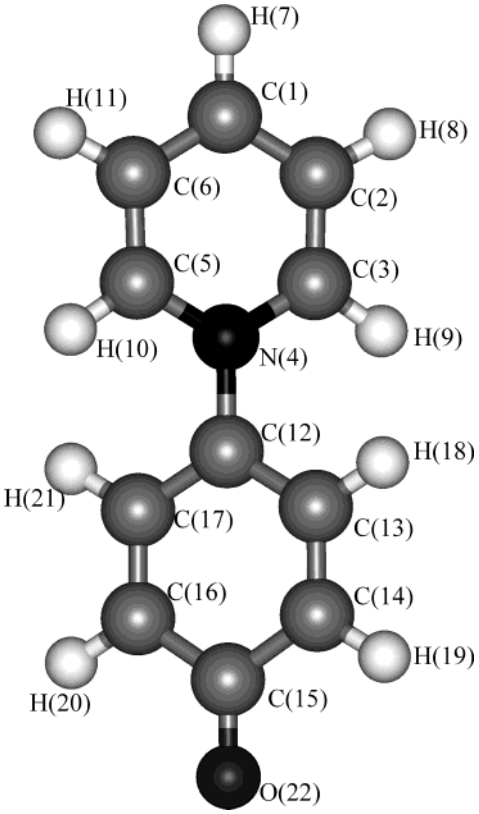

Figure 1. Molecular geometry and atom labelings of pyridinium-*N*-phenoxide betaine (4-(1-pyridinio)phenolate).

intramolecular ET reactions is that reaction occurring in the excited S_1 state of betaine dye molecules. Betaine dye molecules have drawn much attention from both the experimental[19−30] and theoretical communities[31−35] due to their distinct charge-transfer absorption band that depends strongly on solvent polarity and S_1 relaxation via back ET reaction. By use of transient absorption spectroscopy, Barbara and co-workers studied back ET reaction occurring in the betaine-30 molecule.[20−23] McHale and co-workers have studied intramolecular vibrational and solvent motions associated with charge-transfer excitation in the betaine-30 molecule using resonance Raman spectroscopy.[24−26] Werncke et al. investigated vibrational relaxation in the electronic ground state after intramolecular back ET by picosecond time-resolved anti-Stokes Raman spectroscopy.[27−29] Among computational studies on that dye molecule, Mente and Maroncelli carried out simulations of betaine-30 in various solvents to study solvatochromism.[32] Lobaugh and Rossky have investigated the spectroscopy as well as the dynamics of the first excited state of betaine-30[33,34] using mixed quantum/classical dynamics.[36]

In the present study, the simplest betaine, pyridinium-*N*-phenoxide betaine [4-(1-pyridinio)phenolate] is studied. As is shown in Figure 1, the molecule consists of a linked pyridinium ring and a phenoxide ring. The goal is to examine methods for evaluating FC factors for a large molecule with the sum-over-states method and to investigate the properties of FC density functions obtained with different models. We will employ harmonic PES's, as has been used extensively for vibrational or vibronic-spectrum calculations and ET reaction-rate calculations.[37−39] We include a detailed consideration of frequency shifts and Duschinsky rotation, which can play a role in vibrational motions.[10,40−43] This generality allows us to study the importance of frequency shifts and Duschinsky rotation on FC factors. In general, one expects that a torsional motion cannot be described by a harmonic PES due to the softness and periodicity of that coordinate. In most treatment of a torsional motion, a periodic potential energy function for the torsional PES is sought, and the torsional motion is considered as a wave packet evolving on the potential energy function.[44−46] We follow this methodology here, and by doing so, we also study the effect of the torsional motion on FC factors. By comparing FC density functions obtained from the sum-over-states method and the time-dependent method, we will examine the advantages of each method over the other. In particular, we will investigate the behavior of FC factors in the high-frequency region, where the FC density function has contribution from a large number of FC factors.[47]

In experiments on optical spectra in the condensed phase, physical quantities such as reorganization energy can sometimes be obtained by fitting the optical spectra with a simple model.[22] One of the most popular models is due to Jortner,[48] where nuclear degrees of freedom are represented by one classical low-frequency mode and one quantal high-frequency mode. By fitting the FC density function with this model and by comparing the parameters of the model to the exact results, we will investigate how accurately the Jortner model provides access to the physical quantities.

In this paper, we specifically consider the excited state as the initial state and the corresponding emission spectrum. We expect that the main conclusions regarding the usefulness of alternative computational methods and the impact of variations in the harmonic model on the spectra would be similar if the ground-state absorption spectra were considered. This work is organized as follows. In the next section, we discuss theoretical methods for computing FC factors and FC density functions for the harmonic and torsional motions. In section III, the calculated results are shown and discussed. Concluding remarks appear in the final section IV.

II. Theoretical Methods

We begin by considering the ground and the first excited state of the simplest betaine molecule, in the gas phase. Considering ultrafast time scales of intramolecular vibrational motions, we make the reasonable and conventional assumption that the relaxation into the equilibrium geometry in the first excited state occurs rapidly after the electronic excitation.[22] We will primarily use a low-temperature limit for calculations, corresponding to an initial state with the excited-state vibrations all in their ground state.[49,42] The model Hamiltonian of the system composed of these two electronic states can be expressed in terms of mass-weighted normal coordinates $\mathbf{Q} = \{Q_1, Q_2, ..., Q_{3N-6}\}$ where N is the number of atoms in the molecule

$$\hat{H} = |g\rangle\hat{H}_g\langle g| + |e\rangle\hat{H}_e\langle e| + \gamma^\dagger|e\rangle\langle g| + \gamma|g\rangle\langle e| \qquad (1)$$

where $|g\rangle$ denotes the electronic ground state and $|e\rangle$ the first excited state. γ is an electronic coupling matrix element (assumed constant), while $\hat{H}_g$ and $\hat{H}_e$ are the nuclear Hamiltonians on electronic surfaces $|g\rangle$ and $|e\rangle$, respectively

$$\hat{H}_g = \hat{T}(\dot{\mathbf{Q}}_g) + \hat{V}_g(\mathbf{Q}_g) \qquad (2a)$$

$$\hat{H}_e = \hat{T}(\dot{\mathbf{Q}}_e) + \hat{V}_e(\mathbf{Q}_e) \qquad (2b)$$

Here $\hat{T}$ and $\hat{V}$ are the kinetic and the potential energy operators, respectively.

The Golden Rule transition rate from the first excited state to the ground state is expressed with FC factors as[47]

$$k_{ET} = \frac{2\pi\gamma^2}{\hbar}\sum_g FC(e;g)\delta(E_e - E_g) \quad (3)$$

Here $E_{e(g)}$ is the total energy in the first excited (ground) state. $FC(e;g)$ is the FC weight or the squared FC overlap integral for each final state g and is defined as

$$FC(e;g) = I(e;g)^2 = |\langle\chi_e(\mathbf{Q}_e)|\chi_g(\mathbf{Q}_g)\rangle|^2 \quad (4)$$

where $I(e;g)$ is the FC overlap integral and $\chi_{e(g)}(\mathbf{Q}_{e(g)})$ are nuclear vibrational states in the first excited (ground) state. From the practical point of view, FC density functions are more useful than individual FC factors due to the resolution limit. Assuming the lowest vibrational level initially in the first excited state, the FC density functions $\Sigma(\omega)$ can be expressed as[47]

$$\Sigma(\omega) = \frac{1}{\delta\omega}\sum_g I(0;g)^2 \quad (5)$$

where the sum is taken over the vibrational states in the electronic ground state within some energy range $\delta\omega$, namely, $|\omega - \omega^g| \le \delta\omega/2$. Here $\hbar\omega^g$ represents the vibrational energy difference of the ground and the first excited vibronic states. For instance, $\hbar\omega^g = \sum_j n_j^g \hbar\omega_j^g - \Delta G$ for the spin-boson model (no frequency shifts or mode mixing), where n_j^g and ω_j^g are a jth vibrational quantum number and a jth frequency in the ground state, respectively, and ΔG is the potential energy minimum difference between two electronic states.

Up to this point, a general description for the FC density function has been provided. We now invoke some reasonable approximations for the calculation of that function. First, a harmonic PES is utilized for the vibrational motions other than the torsional motion. In many cases, a spin-boson model,[50] which only considers displacements in harmonic potentials, is sufficient to describe a system.[51] In general, however, frequency shifts and mixing of modes (Duschinsky rotation) must be taken into account to precisely explain the change of the vibrational normal modes accompanied by an electronic transition.[42,43] The detailed procedure used to obtain frequency shifts and the Duschinsky rotation matrix is described in detail elsewhere.[51,52] For the highly anharmonic torsional motion, we use a method that has been proposed by Seidner et al.[44] and used popularly by others.[45,46] This method will be described in detail in the second subsection.

We decompose the nuclear Hamiltonian in eq 1 as[53]

$$\hat{H} = \hat{H}^{har} + \hat{H}^{tor} \quad (6)$$

where $\hat{H}^{har}$ means the Hamiltonian which describes all the vibrational motions subject to the harmonic potential approximation and $\hat{H}^{tor}$ represents the Hamiltonian for the torsional motion. Assuming that the torsional motion decouples from the other modes, based on the time scale difference between slow torsional motions and other motions, the FC density function can be written as[7]

$$\Sigma^{tot}(\omega) = \int_{-\infty}^{\infty} d\omega' \Sigma^{har}(\omega - \omega')\Sigma^{tor}(\omega') \quad (7)$$

where $\Sigma^{har}(\omega)$ is the FC density function for $\hat{H}^{har}$ and $\Sigma^{tor}(\omega)$ that for $\hat{H}^{tor}$. Detailed expressions for $\Sigma^{har}(\omega)$ and $\Sigma^{tor}(\omega)$ as well as $\hat{H}^{har}$ and $\hat{H}^{tor}$ are provided next.

TABLE 1: Comparison between the Computational Experimental Data for Low-Frequency, High-Frequency, and Total Intramolecular Reorganization Energies for Simplest Betaine and Betaine-30[a]

	λ_{low}/cm^{-1}	λ_{high}/cm^{-1}	λ_{tot}/cm^{-1}
this work A[b,c]	3057	19011	22068
this work B[b,d]	2130	3100	5230
Barbara[e]	1233	1276	3509
Maroncelli[f]	1100		
Rossky[g]	760		
McHale[h]	33	87	120
Ernsting[i]	1940	1430	3370

[a] Only this work is on the simplest betaine. All the other studies have been carried out on betaine-30. [b] Both methods are using the spin-boson model, and the ground-state frequencies are used. [c] The reorganization energy calculation in this work A is based on the method mentioned as the straightforward method in text. [d] This calculation is based on Lee et al.'s method. [e] Reference 22. [f] Reference 32. [g] Reference 33. [h] Reference 34. [i] Reference 30.

A. Franck−Condon Density Function for Harmonic Motions with Frequency Shifts and Duschinsky Rotation Matrix. We consider $3N - 7$ harmonic vibrational degrees of freedom, with the seventh degree of freedom excluded being the torsional degree of freedom. We use mass-weighted normal coordinates denoted as $\mathbf{Q} = \{Q_1, Q_2, ..., Q_{3N-7}\}$. The harmonic nuclear Hamiltonians in the two states differ by frequency shifts and Duschinsky rotation as well as the displacement of the equilibrium nuclear positions. The Hamiltonian is then given by

$$\hat{H}^{har} = |g\rangle\hat{H}_g^{har}(\mathbf{Q}_g)\langle g| + |e\rangle\hat{H}_e^{har}(\mathbf{Q}_e)\langle e| + \gamma^{har}(|g\rangle\langle e| + |e\rangle\langle g|) \quad (8)$$

where γ^{har} is assumed to be real and static and

$$\hat{H}_g^{har}(\mathbf{Q}_g) = \frac{1}{2}\dot{\mathbf{Q}}_g^T\dot{\mathbf{Q}}_g + \frac{1}{2}\mathbf{Q}_g^T\Omega_g\mathbf{Q}_g \quad (9a)$$

$$\hat{H}_e^{har}(\mathbf{Q}_e) = \frac{1}{2}\dot{\mathbf{Q}}_e^T\dot{\mathbf{Q}}_e + \frac{1}{2}\mathbf{Q}_e^T\Omega_e\mathbf{Q}_e \quad (9b)$$

Here Ω_e and Ω_g are diagonalized frequency matrixes in each state and ΔG is the potential energy minimum difference between the two electronic states. $\mathbf{Q}^T$ is the transpose of $\mathbf{Q}$.

To evaluate a FC overlap integral of $I^{har}(e,g) = \langle\chi_e^{har}(\mathbf{Q}_e)|\chi_g^{har}(\mathbf{Q}_g)\rangle$, we should express the coordinates of the ground state as a function of the coordinates of the first excited state. This can be accomplished by a linear combination[9−51]

$$\mathbf{Q}_g = \mathbf{D}\mathbf{Q}_e + \Delta\mathbf{Q} \quad (10)$$

where $\mathbf{D}$ is the Duschinsky rotation matrix and $\Delta\mathbf{Q}$ means a mass-weighted displacement vector.

As discussed elsewhere, alternative methods to obtain $\mathbf{D}$ and $\Delta\mathbf{Q}$ are available.[51,52] In a method due to Lee et al.,[51] the geometry optimization is only carried out for the initial electronic state and the geometry of the final electronic state is estimated by projecting the force constant matrix (Hessian matrix) at the initial state optimized geometry. Reorganization energies obtained in this way compare favorably to those reorganization energies inferred from experimental and computational data as show in Table 1. In Table 1, it should be noted that the values in the present work are obtained from the simplest betaine and all the others come from the betaine-30. Betaine-30 includes five pendant phenyl rings on the structure of Figure 1. In Table 1, method A corresponds to the

straightforward method where geometry optimizations for each electronic state are performed independently and method B is Lee et al.'s method, just described. Both methods in this work use the spin-boson model for the calculation of the reorganization energy. Compared with experimental data, Lee et al.'s method (method B) provides a far closer value to the experimental results than method A. The need for this less intuitive approach results from relatively large displacements that are observed in the present case for method A, possibly because of the associated large torsional displacement between electronic states. Specifically, we find that the direct approach leads to seven modes between 600 and 1200 cm^{-1} where the magnitude of the calculated displacements obtained from the direct approach are greater than 1.0 and four modes with frequencies greater than 3000 cm^{-1} with calculated displacements greater than 0.5. These eleven modes contribute a reorganization energy of 14 500 cm^{-1} in method A.

Following ref 51, here, we first optimize the excited state and perform frequency analysis of that electronic state to obtain the Ω_e and $3N(3N-7)$ transformation matrix $\mathbf{L}_e^{mx}$, which transforms mass-weighted Cartesian coordinates into normal coordinates. Next we calculate the Hessian matrix and the mass-weighted force vector (gradient) of the ground state at the equilibrium position of the first excited state. The Duschinsky matrix D can then be evaluated from the Hessian matrix of the ground state in Cartesian coordinates.[35] The mass-weighted displacement vector $\Delta\mathbf{Q}$ can then be calculated.

Sharp and Rosenstock have derived a generating-function-based expression for FC factors.[10] Following their method, we reach the equation

$$\sum_{\mathbf{m}=0}^{\infty}\sum_{\mathbf{n}=0}^{\infty}\mathbf{T}^{\mathbf{m}}\mathbf{U}^{\mathbf{n}}\left(\frac{2^{\mathbf{m}}2^{\mathbf{n}}}{\mathbf{m}!\mathbf{n}!}\right)I^{\mathrm{har}}(\mathbf{m},\mathbf{n}) = I^{\mathrm{har}}(\mathbf{0},\mathbf{0})\exp[-(\mathbf{T}^{\mathrm{T}}\mathbf{A}\mathbf{T} + 2\mathbf{T}^{\mathrm{T}}\mathbf{B}) - (\mathbf{U}^{\mathrm{T}}\mathbf{C}\mathbf{U} + 2\mathbf{U}^{\mathrm{T}}\mathbf{G}) + 2\mathbf{T}^{\mathrm{T}}\mathbf{E}\mathbf{U}] \quad (11)$$

where $\mathbf{T}$ and $\mathbf{U}$ are dummy variable vectors.[10]

The matrixes in eq 11 are given as

$$\mathbf{A} = \mathbf{I} - 2\mathbf{J}(\mathbf{J}^{\mathrm{T}}\mathbf{J} + \mathbf{I})^{-1}\mathbf{J}^{T} \quad (12a)$$

$$\mathbf{C} = \mathbf{I} - 2(\mathbf{J}^{\mathrm{T}}\mathbf{J} + \mathbf{I})^{-1} \quad (12b)$$

$$\mathbf{E} = 2(\mathbf{J}^{\mathrm{T}}\mathbf{J} + \mathbf{I})^{-1}\mathbf{J}^{\mathrm{T}} \quad (12c)$$

and vectors as

$$\mathbf{B} = [\mathbf{J}(\mathbf{J}^{\mathrm{T}}\mathbf{J} + \mathbf{I})^{-1}\mathbf{J}^{\mathrm{T}} - \mathbf{I}]\Delta \quad (13a)$$

$$\mathbf{G} = (\mathbf{J}^{\mathrm{T}}\mathbf{J} + \mathbf{I})^{-1}\mathbf{J}^{\mathrm{T}}\Delta \quad (13b)$$

Here $\mathbf{I}$ is the identity matrix, and $\mathbf{J}$ and a dimensionless vector Δ are defined respectively as

$$\mathbf{J} = \Gamma_g\mathbf{D}\Gamma_e^{-1} \quad (14a)$$

$$\Delta = \Gamma_g\Delta\mathbf{Q} \quad (14b)$$

where an element of the diagonal matrix Γ_g is given as

$$(\Gamma_g)_{jj} = \left(\frac{\omega_j^g}{\hbar}\right)^{1/2} \quad (15)$$

In addition, $I^{\mathrm{har}}(\mathbf{0},\mathbf{0})$ in eq 13 is given as

$$I^{\mathrm{har}}(\mathbf{0},\mathbf{0}) = 2^{(3N-7)/2}[\det(\mathbf{J}^{\mathrm{T}}\mathbf{J} + \mathbf{I})]^{-1/2} \times \exp\left[-\frac{1}{2}\Delta^{\mathrm{T}}\Delta + \frac{1}{2}\Delta^{\mathrm{T}}\mathbf{J}(\mathbf{J}^{\mathrm{T}}\mathbf{J} + \mathbf{I})^{-1}\mathbf{J}^{\mathrm{T}}\Delta\right] \quad (16)$$

where $\mathbf{0} = (0_1, 0_2, ..., 0_k, ..., 0_{3N-7})$.

Many conventional methods use the general recursion relation to calculate multidimensional FC overlap integrals.[10-15] In our case, we derive a recursion relations from eq 11, which leads to

$$I^{\mathrm{har}}(\mathbf{m},\mathbf{n}+\mathbf{1}_k) = -\sum_{j=1}^{3N-7} c_{kj}\left(\frac{n_j}{n_k+1}\right)^{1/2} I^{\mathrm{har}}(\mathbf{m},\mathbf{n}-\mathbf{1}_j) - d_k\left(\frac{2}{n_k+1}\right)^{1/2} I^{\mathrm{har}}(\mathbf{m},\mathbf{n}) + \sum_{j=1}^{3N-7} e_{kj}\frac{m_j}{n_k+1}^{1/2} I^{\mathrm{har}}(\mathbf{m}-\mathbf{1}_j,\mathbf{n}) \quad (17)$$

where $\mathbf{n} = (n_1, n_2, n_3, ..., n_{3N-7})$ and $\mathbf{1}_k = (0_1, 0_2, ..., 1_k, ..., 0_{3N-7})$. Since we have assumed that the excited state vibrations are in their ground state (namely, $\mathbf{m} = 0$), eq 17 is simplified into

$$I^{\mathrm{har}}(\mathbf{0},\mathbf{n}+\mathbf{1}_k) = -\sum_{j=1}^{3N-7} c_{kj}\left(\frac{n_j}{n_k+1}\right)^{1/2} I^{\mathrm{har}}(\mathbf{0},\mathbf{n}-\mathbf{1}_j) - d_k\left(\frac{2}{n_k+1}\right)^{1/2} I^{\mathrm{har}}(\mathbf{0},\mathbf{n}) \quad (18)$$

The straightforward recursion relation method requires large amounts of memory, limiting their applications.[11,17] To overcome this problem, Ruhoff and Ratner[17] proposed the TLFBT, which is based on Gruner and Brumer's binary tree algorithm.[11] In Gruner and Brumer's binary tree algorithm, one large binary tree grows to save FC factors. However, the TLFBT method divides the large binary tree into smaller binary trees. Each binary tree is labeled by the level and stores only FC factors belonging to the same level. Here, the level L is defined as

$$L = \sum_{j=1}^{3N-7} n_j \quad (19)$$

where n_j is the quantum number of the jth normal mode. The TLFBT method uses the fact that only the previous two levels $L-1$ and $L-2$ are required to calculate a FC factor in the level L. Therefore, the method stores FC factors pertaining to just the previous two levels, greatly reducing the memory usage. Although the TLFBT algorithm is used for our study, the number of FC integrals to be computed is still large for 59 normal modes. To reduce the number of FC integrals, we modify the TLFBT method and use symmetry groups for vibrational normal modes next.

In general, totally symmetric low-frequency modes have large displacements, and therefore high quantum numbers in the low-frequency modes should be included in the calculation of the FC factors. For totally symmetric high-frequency modes, however, displacements are small and only a few terms in a progression are sufficient. Consider the level L binary tree. In this binary tree, FC factors are computed up to L quanta of each mode. When L is large, the computation of a FC factor for a high-frequency normal mode whose displacement is small wastes time and memory. To address the problem, our modified

method separates modes whose displacements are large from the other modes. First, FC factors for the large displacement modes are calculated, and then the binary trees grow up from each of the FC factors for the large displacement modes. For example, suppose that among totally symmetric modes, we have 4 modes which have large displacements, and we should consider quantum numbers up to N_1, N_2, N_3, and N_4 quanta for the 4 modes, respectively. Then, one first calculates FC factors, the total number of which is $N_1 \times N_2 \times N_3 \times N_4$. Then, level L is decided from the quantum numbers of only the remaining modes, and binary trees grow up from each of the FC factors computed from the 4 modes. We can label each binary tree as (0, 0, 0, 0, 0), (0, 0, 0, 0, 1), ..., (0, 0, 0, 0, L), (1, 0, 0, 0, 0), (1, 0, 0, 0, 1), ..., (1, 0, 0, 0, L), ..., (N_1, N_2, N_3, N_4, L), where the first four numbers in the parenthesis are quantum numbers for the four large displacements modes, and the last number is the level for the other modes. Since we consider the modes whose displacements are large separately, we can keep the level L small.

In addition, we use vibrational symmetry groups of the simplest betaine molecule. Vibrational normal modes in the first excited state belong to A′ and A″ symmetries since the symmetry of the optimized geometry in the first excited state is C_s.[35] Because of the symmetry, the Duschinsky matrix is block diagonalized into two submatrixes. (See Figure 2.) Then, each submatrix can be treated separately, and FC overlap integrals are factored into a product, which is given as

$$I^{\mathrm{har}}(\mathbf{0},\mathbf{n}) = I^{\mathrm{har}}(\mathbf{0},\mathbf{n}^{\mathrm{A}'}) \times I^{\mathrm{har}}(\mathbf{0},\mathbf{n}^{\mathrm{A}''}) \tag{20}$$

Here $\mathbf{n}^{\mathrm{A}'}$ is defined as $\mathbf{n}^{\mathrm{A}'} = (n_1^{\mathrm{A}'}, ..., n_{N_{\mathrm{A}'}}^{\mathrm{A}'})$ and $\mathbf{n}^{\mathrm{A}''} = (n_1^{\mathrm{A}''}, ..., n_{N_{\mathrm{A}''}}^{\mathrm{A}''})$; $N_{\mathrm{A}'}$ and $N_{\mathrm{A}''}$ are the total number of modes pertaining to symmetric groups A′ and A″, respectively.

Under the assumption that the excited-state vibrations are all in their ground state, the FC density function is now given as[47]

$$\Sigma^{\mathrm{har}}(\omega) = \frac{1}{\delta\omega}\sum_k I^{\mathrm{har}}(\omega^{\mathrm{g}})^2 \tag{21}$$

where the sum is taken over the vibrational states in the electronic ground state within a resolution $\delta\omega$, i.e., $|\omega - \omega^{\mathrm{g}}| \le \delta\omega/2$ and ω^{g} is defined as

$$\hbar\omega^{\mathrm{g}} = \sum_{j=1}^{3N-7} n_j^{\mathrm{g}}\hbar\omega_j^{\mathrm{g}} + \hbar\Delta w_{\mathrm{ge}}^{\mathrm{zpe}} - \Delta G \tag{22}$$

Here $\Delta\omega_{\mathrm{ge}}^{\mathrm{zpe}}$ is the zero point energy difference between the ground and the first excited state, that is, $\Delta\omega_{\mathrm{ge}}^{\mathrm{zpe}} = \omega_{\mathrm{g}}^{\mathrm{zpe}} - \omega_{\mathrm{e}}^{\mathrm{zpe}}$.

B. Franck−Condon Density Function Induced by Torsional Motion. As mentioned above, the central inter-ring torsional motion is well beyond a harmonic potential description, and the method introduced in the previous section cannot be applied to this torsional motion. The alternative time-dependent method due to Heller et al.,[6,7] yields the FC density function via a Fourier transform of the time-dependent overlap between two nuclear wave functions evolving on two different electronic PES's.

Following Heller's method,[6,7] first we explicitly calculate the periodic torsional potential energy function for the torsional motion of the electronic ground state. The torsional dynamics is then described as a wave packet evolving on the periodic PES. The dynamics of that mode is obtained by solving directly the time-dependent Schrödinger equation (TDSE), as discussed elsewhere.[35,44,45,46]

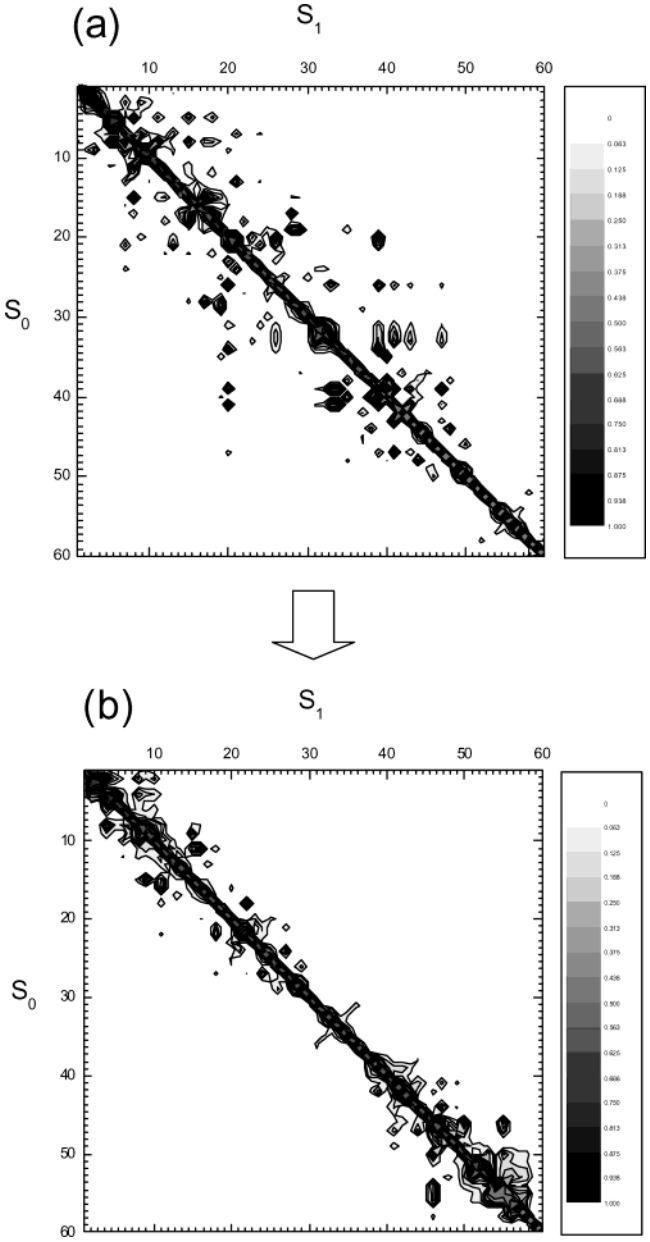

Figure 2. Absolute values of Duschinsky matrixes' elements. (a) Normal modes in the ground (S_0) and the first excited state (S_1) are arranged in terms of increasing order of frequencies. (b) Same as (a) except for being sorted by symmetry first and then by frequency within the same symmetry. In (b), the modes 1−37 belong to symmetry A′ and 38−60 to symmetry A″.

The initial nuclear wave function is in the equilibrium position of the first excited state, so that the harmonic potential can be used for the first excited-state PES $V_{\mathrm{e}}^{\mathrm{tor}}(\theta)$ given as

$$V_{\mathrm{e}}^{\mathrm{tor}}(\theta) = \frac{1}{2} I^{\mathrm{tor}}(\omega_{\mathrm{e}}^{\mathrm{tor}})^2(\theta - \theta_0{}^{\mathrm{e}})^2 \tag{23}$$

where θ_0^{e} is the torsional angle at the equilibrium configuration of the first excited state. The explicit torsional PES for the ground state is necessary. In general, the PES for the torsional motion is given as[54]

$$V_{\mathrm{g}}^{\mathrm{tor}}(\theta) = \frac{1}{2}\sum_n V_n(1 - \cos\{n(\theta - \theta_0{}^{\mathrm{g}})\}) \tag{24}$$

where $\theta_0{}^{\mathrm{g}}$ is the torsional angle at the equilibrium configura-

tion of the ground state and n is an integer. We obtain parameters for the ground-state torsional PES by fitting computed potential energies as a function of θ.

The FC density can be expressed as the Fourier transform of the overlap between the two nuclear wave functions evolving on the first excited and ground state[6,7]

$$\Sigma^{\mathrm{tor}}(\omega) = 2\mathrm{Re}\int_0^T \mathrm{d}t\langle\Psi_{\mathrm{e}}^{\mathrm{tor}}(t)|\Psi_{\mathrm{g}}^{\mathrm{tor}}(t)\rangle \exp(i\omega t) \quad (25)$$

where $\Psi_{\mathrm{e}}^{\mathrm{tor}}(t)$ and $\Psi_{\mathrm{g}}^{\mathrm{tor}}(t)$ are nuclear wave functions on the first excited and ground states, respectively, where $\Psi_{\mathrm{e}}^{\mathrm{tor}}(0) = \Psi_{\mathrm{g}}^{\mathrm{tor}}(0)$. The relation between τ in eq 25 and $\delta\omega$ in eq 21 is

$$\delta\omega = \frac{2\pi}{\tau} \quad (26)$$

III. Results and Discussion

Geometry optimization and frequency analysis are performed with the Gaussian 98 program.[55] Configuration-interaction singles (CIS) with the 6-31G* basis set is used to optimize the first excited state. The calculations of the Hessian matrix and the gradient of the ground state at the optimized geometry of the first excited state are carried out at the Hartree−Fock level with the same basis set. Frequencies in this paper are scaled with the factor of 0.91.[56] The geometry optimization of the first excited state is performed without applying any symmetry at first. As the torsional angle between the pyridinium ring and the phenoxide ring obtained in this case was found to be very close to 90° and the symmetry very nearly C_s, we proceeded by enforcing C_s symmetry in the first excited state to simplify the following analysis. The torsional angle is thus fixed at 90°; the electronic energy under symmetry was not significantly different from that without symmetry.

Figure 2 shows Duschinsky rotation matrixes ordered by frequency (Figure 2a) and after the blocking by vibrational symmetry groups (Figure 2b). The first 37 normal modes belong to A′, and the other 23 to A″, yielding the block-diagonalized Duschinsky matrix in Figure 2b. Table 2 provides the frequencies and displacements that pertain to A′ and A″. Note that the normal modes pertaining to A″ symmetry group have zero displacements. Before going further, it it worth commenting on the relation between these results and experimental resonance Raman observations.[24−26] Because we consider a simpler related dye, a quantitative comparison is not possible. Experiments on betaine-30 in solvent showed that approximately 19 modes were resonance Raman active, among which 7 modes have prominent displacements (larger than 0.1).[26] Our study shows 18 normal modes whose displacements are relatively large (larger than 0.2). Among them, 9 modes have significant displacements larger than 0.5. On the basis of this observation, our study is in qualitative agreement with the resonance Raman study. Another point of contact between our computational study and the resonance Raman experiments is about the relationship between frequencies and displacements. Both show that displacements in the low-frequency region are in general larger than in the high-frequency region.

Figure 3 shows $\Sigma^{\mathrm{har}}(\omega)$ for harmonic motions with varying resolution $\delta\omega$ (see eq 5). Frequency shifts and Duschinsky rotation are taken into account in the FC density spectra. Zero frequency in the graph corresponds to the minimum energy difference between the ground and first excited-state PES's, i.e., zero corresponds to an adiabatic energy difference of $\Delta G =$ 19 841 cm^{-1} (see eq 11). The total number of FC factors computed is about 5.34×10^{14}, and the sum of FC factors is 0.9845. As quantum numbers increase or the level increases, the number of FC factors to be computed increases rapidly. The sharp increase makes it difficult to obtain all contributing FC factors in the high-frequency region (or high quantum number),

TABLE 2: 60 Normal-Mode Frequencies (cm^{-1}) and Displacements in the Ground and the First Excited State[a,b]

mode	ω_{g}	ω_{e}	ΔQ	mode	ω_{g}	ω_{e}	ΔQ
1	69.5	28.1	−5.69	31	3092.9	3087.0	0.05
2	282.6	201.5	1.56	32	3076.7	3102.3	0.06
3	294.4	280.0	0.21	33	3074.8	3102.8	0.00
4	512.1	387.5	−0.36	34	3104.3	3119.7	−0.04
5	435.7	457.0	−0.75	35	3107.0	3121.4	0.06
6	556.5	538.3	0.19	36	3145.5	3128.4	0.02
7	616.0	594.8	0.06	37	3181.5	3158.7	0.06
8	683.7	631.1	−0.39	38	27.1	62.4	0.00
9	804.7	658.3	0.08	39	56.5	121.6	0.00
10	699.4	692.2	0.39	40	154.0	170.5	0.00
11	1000.7	720.8	−0.05	41	369.2	352.0	0.00
12	765.9	771.3	0.51	42	402.6	425.5	0.00
13	936.3	953.1	0.28	43	410.0	434.9	0.00
14	949.4	969.2	−0.54	44	466.1	544.0	0.00
15	1047.3	972.7	0.19	45	620.1	635.3	0.00
16	1006.6	999.4	0.36	46	874.1	737.2	0.00
17	1018.6	1008.2	−1.01	47	686.4	745.1	0.00
18	1061.5	1097	0	48	768.4	810.9	0.00
19	1145.5	1163	−0	49	838.9	876.7	0.00
20	1201.2	1206	0	50	1025.9	969.0	0.00
21	1266.3	1252.0	−0.03	51	966.6	1018.7	0.00
22	1172.1	1285.0	0.03	52	960.8	1020.8	0.00
23	1327.2	1344.0	−0.59	53	1155.1	1031.4	0.00
24	1452.5	1427.2	0.03	54	1115.2	1081.7	0.00
25	1436.2	1447.7	−0.30	55	901.7	1261.8	0.00
26	1477.6	1478.4	0.29	56	1480.6	1291.5	0.00
27	1528.0	1535.8	0.06	57	1337.5	1370.0	0.00
28	1622.7	1620.2	0.02	58	1522.8	1522.7	0.00
29	1670.2	1666.6	−0.99	59	3094.6	3089.1	0.00
30	1748.3	1746.3	0.30	60	3179.7	3154.4	0.00

[a] CIS with 6-31G* is used to perform a geometry optimization for the first excited state. The frequencies of the ground state are obtained at the optimized geometry of the first excited state by the diagonalizing force constant matrix (Hessian matrix) of the ground state. Calculation for the force constant matrix is performed at the Hartree−Fock level with 6-31G*. Frequency scaling factor is 0.91, and displacements are unitless. See text. [b] The first 37 normal modes belong to the totally symmetric group, A', and the other 23 to the nontotally symmetric group, A''. Note that only the normal modes belonging to A' have nonzero displacements.

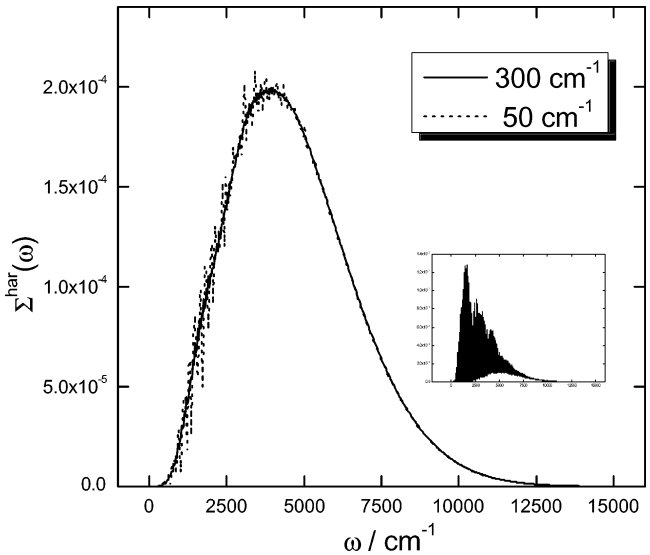

Figure 3. FC densities for the harmonic motions with resolution of 300 and 50 cm^{-1}. The inset shows the FC density with resolution of 1 cm^{-1}. Both frequency shifts and Duschinsky rotation are included.

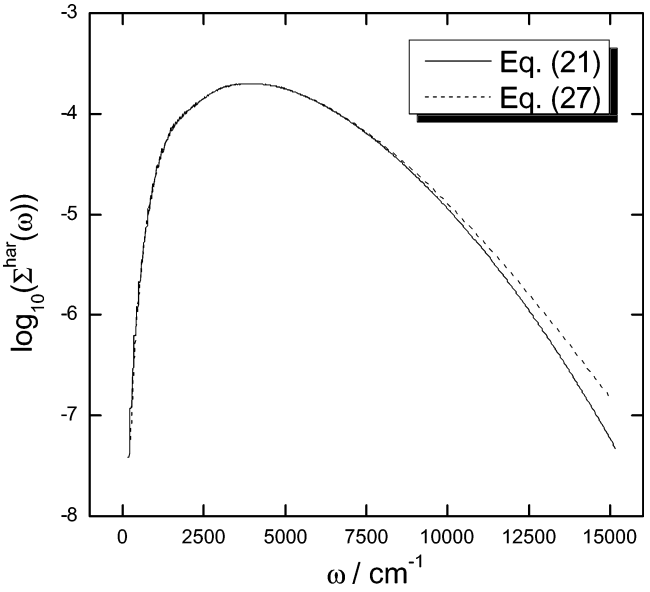

Figure 4. Semilogarithmic plot for the FC density functions comparing between the sum-over-states method and the time-dependent method for the harmonic motions. Both frequency shifts and Duschinsky rotation are included, and $\delta\omega = 300$ cm^{-1}.

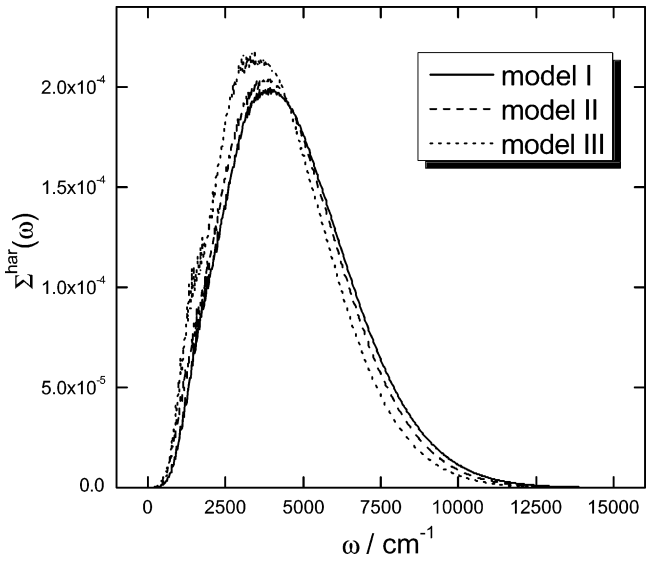

Figure 5. Comparison among several models for $\Sigma^{har}(\omega)$. Model I includes Duschinsky rotation and frequency shifts as well as displacements. In model II, Duschinsky rotation is not considered. Model III only has the effect of displacements. $\delta\omega = 300$ cm^{-1}.

and as a result, the total sum of FC factors is not exactly 1. As $\delta\omega$ becomes small, more fine structure appears in the FC density function. It is interesting to note that, at higher resolution, we can see irregular structure in the low-frequency region, reflecting mode selectivity.[47] Mode selectivity occurs since only a few number of modes can contribute in the low-frequency region. A distinct high-frequency tail is also observed to be discussed later.

A FC density function for the harmonic motions can be also obtained from the Fourier transform of nuclear overlap/phase function (NOPF), i.e., with the time-dependent method outlined above.[6−8] The NOPF for the harmonic motion $J^{har}(t)$ is obtained analytically from the generating function method developed by Kubo−Toyozawa.[38] Then the FC density function can be directly calculated as

$$\Sigma^{har}(\omega) = 2\mathrm{Re}\int_0^\infty \mathrm{d}t J^{har}(t)\exp(i\omega t) \qquad (27)$$

where $J^{har}(t)$ is the NOPF for the harmonic motions.[35] In Figure 4, we show semilogarithmic plots of FC density function from the sum-over-states method and from the time-dependent method for the harmonic motions. Both frequency shifts and Duschinsky rotation are included in both cases, and $\delta\omega$ is 300 cm^{-1}.

$\delta\omega$ of 300 cm^{-1} corresponds to a τ (see eq 26) of 111 fs. For this τ, $|J^{har}(t)| \approx 9.8 \times 10^{-7}$. This small value of $|J^{har}(t)|$ implies that an accurate calculation of the FC density function from the time-dependent method requires determination of $J(t)$ with high accuracy even in regimes of very small amplitude. For higher resolution of $|J^{har}(t)|$ in the time-dependent method, τ should be much larger, and because of the phase recurrence mentioned in the previous study,[35] the values of $|J^{har}(t)|$ in fact increase again and numerical difficulty decreases. Then the time-dependent method can provide an acceptable result even in high resolution provided that the exact expression for $J(t)$ is used.[35,38,51] In the low-frequency region, the sum-over-states method shows a little mode selectivity, but the time-dependent method with low resolution does not. In the high-frequency region, however, due to truncation in the calculation of FC factors in the sum-over-states method, the result from the sum-over-states method becomes inaccurate and we can see the discrepancy between two methods. The sum-over-states method is not restricted by resolution since one actually computes FC factors, and we can control the resolution to whatever extent we want. But that method becomes intractable for large molecules of low symmetry and has difficulty in the calculation of FC factors in the high-frequency region. On the other hand, the time-dependent method is highly efficient in that the method takes less time to compute the FC density function. In addition, the time-dependent method can be readily used for the anharmonic PES.[5] However, it cannot provide individual FC factors. It also depends on the resolution and can suffer from the numerical instability in higher resolution due to the small values of $|J^{har}(t)|$ at increasing times. Thus the two approaches have complementary strengths.

In Figure 5, we show $\Sigma^{har}(\omega)$. Model I includes the effect of Duschinsky rotation as well as frequency shifts and displacements. While frequency shifts and displacements are considered in model II, model III accounts solely for the effect of displacements (spin-boson model). It is evident from Figure 5 that model II is somewhat different from model III, the differences originating from frequency shifts in the model II. A comparison between model I and model II shows that Duschinsky rotation has a relatively minor effect. On the basis of these observations, in our molecular system, frequency shifts introduce larger deviations from the spin-boson model than the Duschinsky rotation does.

It is evident that both frequency shifts and Duschinsky rotation increase values of the FC density function in the high-frequency region. One reason is that nontotally symmetric modes, which have no displacements, can now affect the FC density function through frequency shifts and Duschinsky rotation.[41,42] Sando et al.[42] studied the effects of Duschinsky rotation on an ET rate in a model system where two modes without displacements are mixed among eight modes. They also observed the increased contribution to the ET rate from the high-frequency region, and attributed the increase to the participation of the nontotally symmetric modes. We note that, as frequency shifts and Duschinsky rotation are included, the number of FC factors to be computed is increased; i.e., the total number of FC factors goes from 8.86×10^{10} in model III to 9.66×10^{12}

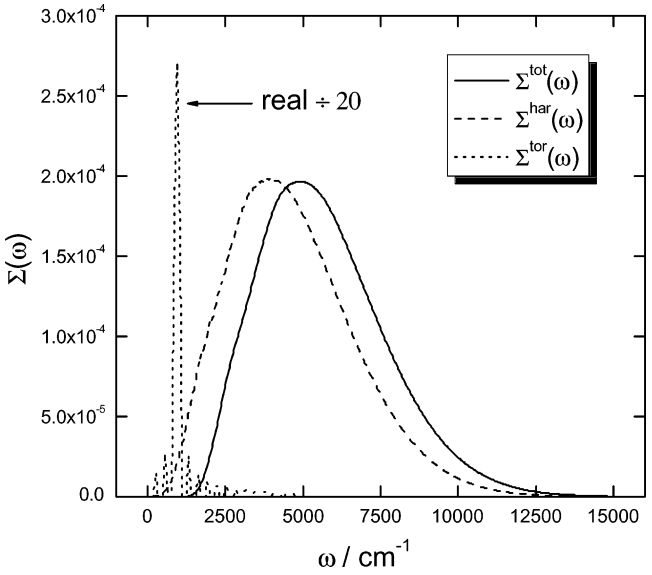

Figure 6. The total FC density, $\Sigma^{tot}(\omega)$, along with $\Sigma^{har}(\omega)$ and $\Sigma^{tor}(\omega)$. Both frequency shifts and Duschinsky rotation are included for $\Sigma^{har}(\omega)$, and $\delta\omega = 300$ cm^{-1}.

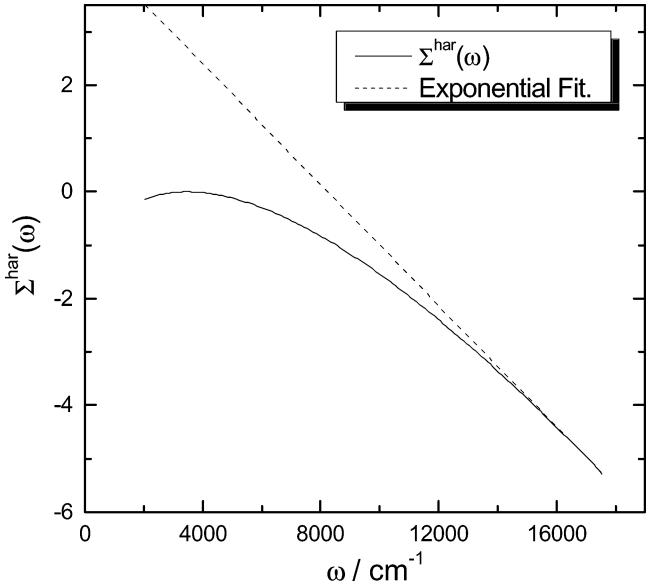

Figure 7. Semilogarithmic plot for the FC density function for the spin-boson model and exponential fit in the high-frequency region to test exponential decay. $\delta\omega = 300$ cm^{-1}.

in model II to 5.34×10^{14} in model I. This increase also reflects the participation of nontotally symmetric modes.

As mentioned previously, under the assumption of separable torsion from the other motions, the total FC density can be written as[7]

$$\sum^{tot}(\omega) = \int_{-\infty}^{\infty} d\omega' \sum^{har}(\omega - \omega') \sum^{tor}(\omega') \quad (28a)$$

$$= \int_{-\infty}^{\infty} d\omega' \sum^{har}(\omega') \sum^{tor}(\omega - \omega') \quad (28b)$$

Figure 6 shows the total FC density function as well as the FC density functions for the harmonic motions and for the torsional motion. The effects of frequency shifts and Duschinsky rotation are included. The calculation of the total FC density function is based on both the sum-over-states method and the time-dependent method. That is to say, the calculation of the FC density function for the harmonic motions are performed using eq 21 and the FC density for the torsional motion is computed based on eq 25. The resolution is 300 cm^{-1}. It is clear that the role of the slow torsional motion is essentially to simply shift the peak of the spectra into a higher position. This is because the $\Sigma^{tor}(\omega)$ in Figure 6 is nearly a delta function, and when $\Sigma^{tor}(\omega) \approx \delta(\omega - \omega_0)$, $\Sigma^{tot}(\omega)$ in eq 28a becomes $\Sigma^{tot}(\omega) \approx \Sigma^{har}(\omega - \omega_0)$.

One potentially interesting feature of the FC density function is the behavior of the function in the high-frequency (or energy) region.[57,58] Englman and Jortner showed that an exponential decay of the FC function can be expected from the spin-boson model in the weak coupling limit, defined as $\lambda_v \leq \hbar\langle\omega\rangle$.[58] Here the vibrational reorganization energy λ_v is given for harmonic model as

$$\lambda_v = \sum_j^{3N-6} \frac{1}{2} \Delta_j^2 \hbar\omega_j \quad (29)$$

and the mean vibrational frequency $\langle\omega\rangle$ is

$$\langle\omega\rangle = \frac{\sum_j^{3N-6} \omega_j}{3N-6} \quad (30)$$

In Figure 7, we present a semilogarithmic plot of the FC density function to examine the high-frequency behavior in our system, also for the spin-boson model (model III). For this purpose, we use the Fourier transform of the NOPF to obtain the FC density function accurately at very high frequency. We also use the spin-boson model to obtain the reorganization easily. In Figure 7, we observe only a roughly exponential decay at very high energy. According to Englman and Jortner's work, to observe a true exponential decay, the vibrational reorganization energy should be equal to or less than the mean vibration frequency. However, the vibrational reorganization energy of 4228 cm^{-1} in our system is much larger than the mean vibrational frequency of 1233 cm^{-1}. Because of the much larger reorganization energy than the mean vibrational frequency, our system falls into the strong coupling limit, where the vibrational reorganization energy is larger than the mean vibrational frequency.

In experiments carried out at room, or high, temperature, fitting functions are frequently used to obtain physical quantities such as reorganization energy from experimental optical spectra. One of the most popular fitting functions is based on the Jortner's expression.[48] In that expression, the description of many nuclear degrees of freedom is simplified to two representative degrees of freedom. One is a low-frequency vibrational mode describing classical motions, and the other is a high-frequency vibrational mode representing quantum mechanical vibrational motions. The resulting model FC density function can be written as[22,48]

$$\Sigma^{har}(\omega) \propto \sum_{k=0}^{\infty} \frac{s^k}{k} \exp\left[- \frac{(\hbar\omega - (\lambda_{cl}^{har} - \Delta G + k\hbar\omega_{qm}))^2}{4\lambda_{cl}^{har} k_B T} \right] \quad (31)$$

Here s is a Huang−Rhys factor $s = \Delta^2/2$ where Δ is the displacement for the high-frequency mode, λ_{cl}^{har} is a classical reorganization energy, which comes from the low-frequency mode, and ω_{qm} is a frequency for the high-frequency quantal mode. The quantum mechanical reorganization energy is determined with the relation $\lambda_{qm}^{har} = s\hbar\omega_{qm}$. Note that, in eq 31, we consider only the FC density function for the harmonic motions, not the total FC density function, for the following reason. It is clear that the FC density function for the torsional

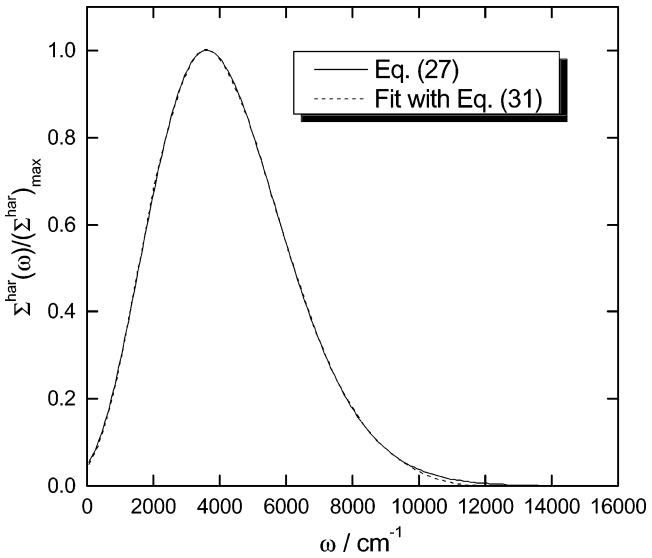

Figure 8. Comparison between the normalized $\Sigma^{har}(\omega)$ from the spin-boson model and fitting with Jortner's model,[48] eq 31. The temperature is held at 298 K. and ΔG is set to zero.

motion in the room temperature is nearly Gaussian due to its low frequency or slow motion (static modulation limit). Since $\Sigma^{har}(\omega)$ in eq 31 is a linear combination of the Gaussian functions and the total FC density function is a convolution of the FC density functions for the harmonic and the torsional motions (see eq 28a), the total FC density function is exactly same as eq 31 except for the replacement of λ_{cl}^{har} by λ_{cl}^{tot}, where $\lambda_{cl}^{tot} = \lambda_{cl}^{har} + \lambda^{tor}$. Since we already know the λ^{tor}, it suffices to consider solely the FC density function for the harmonic motions. Barbara and co-workers[20,22,23] used eq 31 to obtain the spectroscopic parameters required to calculate back ET reaction rates in a betaine-30 molecule. They fitted the static absorption spectra of the betaine-30 in various solvents with eq 31 and calculated back ET reaction rates with the parameters obtained.

We test the Jortner's model by fitting our exact FC density function with eq 38. Figure 8 shows $\Sigma^{har}(\omega)$ and the fit. The temperature is fixed at 298 K since most experiments on betaine molecules are carried out at this temperature. For the calculation of a thermally averaged $\Sigma^{har}(\omega)$, the time-dependent method of eq 27 and Kubo−Toyozawa formalism for the thermally averaged NOPF[38] are used. In the calculation of $\Sigma^{har}(\omega)$ and the fitting function, ΔG is set to zero. The fitting function in Figure 8 corresponds to the parameters $\lambda_{cl}^{har} = 2004$ cm^{-1}, $s = 1.50$, $\omega_{qm} = 1483$ cm^{-1}, and therefore $\lambda_{qm}^{har} = 2225$ cm^{-1}. Then the total reorganization energy for the harmonic motion from the fitting function is 4229 cm^{-1}. By comparison of this reorganization energy to the reorganization energy of 4228 cm^{-1} for the harmonic motions from the spin-boson model, we find that the Jortner's expression correctly represents the reorganization energy. The frequency for the quantal mode $\omega_{qm} = 1483$ cm^{-1} is comparable to the high frequency of 1554−1800 cm^{-1} obtained from the absorption spectra of a betaine-30 in various solvents with the same fitting function by Barbara and co-workers.[22] To compare the classical and quantum mechanical reorganization energies from the Jortner's expression to the reorganization energies from the spin-boson model, we should divide 60 vibrational normal modes into two groups, low-frequency modes and high-frequency modes. We choose as a separation frequency 300 cm^{-1} by which we can separate low-frequency modes from high-frequency modes.[59] We believe that 300 cm^{-1} as a separation frequency is reasonable since the thermal energy at 298 K is 207 cm^{-1}. The mean low freqeuncy $\langle\omega\rangle_{low} = 147$ cm^{-1} and $\langle\omega\rangle_{high} = 1354$ cm^{-1}. The latter is qualitatively similar to the fitting parameter $\omega_{qm} = 1483$ cm^{-1}, and to the single-mode model parameter of 1554 cm^{-1} determined in ref 22. The exact low-frequency and the high-frequency reorganization energies from the spin-boson model can be calculated from Table 2, and the values are 1476 and 2752 cm^{-1}, respectively. Since the selection of the separation frequency is somewhat arbitrary, the separation of the 60 normal modes into two groups is subtle. Nevertheless, we can see the qualitative agreement between the exact values and the fitting parameters for the reorganization energies.

IV. Concluding Remarks

In this study, FC factors and FC density functions for the 60 vibrational modes of the simplest betaine molecule have been calculated by combination of the sum-over-states method and the time-dependent method. In the sum-over-states method for the 59 harmonic motions, we were able to address the memory overflow problem by modifying the TLFBT algorithm and using the vibrational symmetry groups. The sum-over-states method agrees well with the time-dependent method except for the very high frequency region. Here, the rapid increase of the number of FC factors to be computed prevents a reasonable computation of all the FC factors required. In the low-frequency region, the sum-over-states method reveals a fine structure reflecting some mode selectivity. Compared with experimental data from the resonance Raman experiments, displacement calculations in our study are in qualitative agreement with the experimental results. Both our study and the resonance Raman study show that low-frequency modes have larger displacements than high-frequency modes.

The inclusion of frequency shifts and Duschinsky rotation vastly increases the number of FC factors to be computed in the high-frequency region. As a result, the FC density function becomes broader compared with the simple spin-boson model. We also observed that frequency shifts have more influence on the FC density function than Duschinky rotation. The FC density function for the torsional motion has nearly a delta-function-like shape, and so its role is to shift the position of the FC density function to a higher frequency. This is associated with the slow dynamics of torsion.

In the high-frequency region, we did not observe clear exponential decay. For the simplest betaine molecule, the relatively large structural change between the ground and the first excited state leads to large displacements and the resulting large reorganization energy. As a result, the molecule falls into the strong coupling limit, and an exponential decay energy gap law does not pertain.

When the low-frequency region of FC density function for a large molecule is investigated, we find that the sum-over-states method readily provides fine structures. Because of the rapid increase in the number of contributing FC factors in the high-frequency region and the resulting difficulty of computation, however, the sum-over-states method does not provide accurate values. In this case, the time-dependent method is an excellent alternative.

The FC density function for the harmonic motions in the spin-boson model is well fitted by the Jortner expression.[48] The total reorganization energy obtained from the fit is in excellent agreement with the reorganization energy in the spin-boson model. From this fit, we can also see that the physical parameters, such as low- and high-frequency components of the reorganization energy, and the characteristic frequencies are in qualitative agreement only, as might be expected.

Acknowledgment. The support of this research by a grant from the National Science Foundation (CHE-0134775) and the R. A. Welch Foundation is gratefully acknowledged.

References and Notes

(1) Bolton, J. R.; Mataga, N.; MeLendon, G. In *Electron Transfer in Inorganic, Organic, and Biological Systems*; Bolton, J. R., Mataga, N., MeLendon, G., Eds.; American Chemical Society: Washington, DC, 1991.
(2) Bixon, M.; Jortner, J. In *Electron Transfer-From Isolated Molecules to Biomolecules*; Jortner, J., Bixon, M., Eds.; John Wiley & Sons: New York, 1999.
(3) Condon, E. U. *Phys. Rev.* **1928**, *32*, 858.
(4) Manneback, C. *Physica* **1951**, *17*, 1001.
(5) Myers, A. B. In *Biological Application of Raman Spectroscopy*; Spiro, T. G., Ed.; Wiley: New York, 1987; Vol. 2.
(6) Heller, E. J. *J. Chem. Phys.* **1978**, *68*, 2066.
(7) Heller, E. J. *J. Chem. Phys.* **1978**, *68*, 3891.
(8) Lee, S.-Y.; Heller, E. J. *J. Chem. Phys.* **1979**, *71*, 4777.
(9) Duschinsky, F. *Acta Physicochim.* **1937**, *7*, 551.
(10) Sharp, T. E.; Rosenstock, H. M. *J. Chem. Phys.* **1964**, *41*, 3453.
(11) Gruner, D.; Brumer, P. *Chem. Phys. Lett.* **1987**, *138*, 310.
(12) Lermé, J. *Chem. Phys.* **1990**, *145*, 67.
(13) Ruhoff, P. T. *Chem. Phys.* **1994**, *186*, 355.
(14) Peluso, A.; Santoro, F.; Re, G. D. *Int. J. Quantum Chem.* **1997**, *63*, 233.
(15) Malmqvist, P.; Forsberg, N. *Chem. Phys.* **1989**, *228*, 227.
(16) Iachello, F.; Ibrahim, M. *J. Phys. Chem. A* **1998**, *102*, 9427.
(17) Ruhoff, P. T.; Ratner, M. A. *Int. J. Quantum Chem.* **2000**, *77*, 383.
(18) Toniolo, A.; Persico, M. *J. Comput. Chem.* **2001**, *22*, 968.
(19) Reichardt, C. *Angew. Chem., Int. Ed. Engl.* **1979**, *18*, 98.
(20) Åkesson, E.; Walker, G. C.; Barbara, P. F. *J. Chem. Phys.* **1991**, *95*, 4188.
(21) Barbara, P. F.; Walker, G. C.; Smith, T. P. *Science* **1992**, *256*, 975.
(22) Walker, G. C.; Åkesson, E.; Johnson, A. E.; Levinger, N. E.; Barbara, P. F. *J. Phys. Chem.* **1992**, *96*, 3728.
(23) Reid, P. J.; Barbara, P. F. *J. Phys. Chem.* **1995**, *99*, 3554.
(24) Zong, Y.; McHale, J. L. *J. Chem. Phys.* **1997**, *106*, 4963.
(25) Zong, Y.; McHale, J. L. *J. Chem. Phys.* **1997**, *107*, 2920.
(26) Zhao, X.; Burt, J. A.; Knorr, F. J.; McHale, J. L. *J. Phys. Chem. A* **2001**, *105*, 11110.
(27) Hogiu, S.; Werncke, W.; Pfeiffer, M.; Elsaesser, T. *Chem. Phys. Lett.* **1999**, *312*, 407.
(28) Hogiu, S.; Dreyer, J.; Pfeiffer, M.; Brzezinka, K.-W.; Werncke, W. J. *Raman Spectrosc.* **2000**, *31*, 797.
(29) Hogiu, S.; Werncke, W.; Pfeiffer, M.; Elsaesser, J. D. T. *J. Chem. Phys.* **2000**, *113*, 1587.
(30) Kovalenko, S. A.; Eilers-König, N.; Senyushkina, T. A.; Ernsting, N. P. *J. Phys. Chem. A* **2001**, *105*, 4834.
(31) Bartkowiak, W.; Lipiński, L. *J. Phys. Chem. A* **1998**, 5236.
(32) Mente, S. R.; Maroncelli, M. *J. Phys. Chem. B* **1999**, *103*, 7704.
(33) Lobaugh, J.; Rossky, P. J. *J. Phys. Chem. A* **1999**, *103*, 9432.
(34) Lobaugh, J.; Rossky, P. J. *J. Phys. Chem. A* **2000**, *104*, 899.
(35) Hwang, H.; Rossky, P. J. *J. Phys. Chem. B* In press.
(36) Tully, J. C. *J. Chem. Phys.* **1990**, *93*, 1061.
(37) Wilson, J. E. B.; Decius, J. C.; Cross, P. C. *Molecular Vibrations*; McGraw-Hill: New York, 1955.
(38) Kubo, R.; Toyozawa, Y. *Prog. Theor. Phys.* **1955**, *13*, 160.
(39) Levine, I. N. *Molecular spectroscopy*; John Wiley & Sons: New York, 1975.
(40) Small, G. J. *J. Chem. Phys.* **1971**, *54*, 3300.
(41) Mebel, A. M.; Hayashi, M.; Liang, K. K.; Lin, S. H. *J. Phys. Chem. A* **1999**, *103*, 10674.
(42) Sando, G. M.; Spears, K. G.; Hupp, J. T.; Ruhoff, P. T. *J. Phys. Chem.* **2001**, *105*, 5317.
(43) Sando, G. M.; Spears, K. G. *J. Phys. Chem.* **2001**, *105*, 5326.
(44) Seidner, L.; Domcke, W. *Chem. Phys.* **1994**, *186*, 27.
(45) Chuang, Y.; Truhlar, D. G. *J. Chem. Phys.* **2000**, *112*, 1221.
(46) Clary, D. C. *J. Chem. Phys.* **2001**, *114*, 9725.
(47) Bixon, M.; Jortner, J. *Chem. Phys.* **1993**, *176*, 467.
(48) Jortner, J. *J. Chem. Phys.* **1976**, *64*, 4860.
(49) Karabunarilev, S.; Baumgarten, M.; Bittner, E. R.; Müllen, K. *J. Chem. Phys.* **2000**, *113*, 11372.
(50) Leggett, A. J.; Chakravarty, S.; Dorsey, A. T.; Fisher, M. P.; Garg, A.; Zwerger, W. *Rev. Mod. Phys.* **1987**, *59*, 1.
(51) Lee, E.; Medvedev, E. S.; Stuchebrukhov, A. A. *J. Chem. Phys.* **2000**, *112*, 9015.
(52) Mebel, A. M.; Chen, Y.-T.; Lin, S.-H. *Chem. Phys. Lett.* **1996**, *258*, 53.
(53) Köppel, H.; Domcke, W.; Cederbaum, L. S. *Adv. Chem. Phys.* **1984**, *57*, 59.
(54) Sinclair, W. E.; Yu, H.; Phillips, D. *J. Chem. Phys.* **1997**, *106*, 5797.
(55) Frisch, M. J.; Trucks, G. W.; Schlegel, H. B.; Scuseria, G. E.; Robb, M. A.; Cheeseman, J. R.; Zakrzewski, V. G.; Montgomery, J. A., Jr.; Stratmann, R. E.; Burant, J. C.; Dapprich, S.; Millam, J. M.; Daniels, A. D.; Kudin, K. N.; Strain, M. C.; Farkas, O.; Tomasi, J.; Barone, V.; Cossi, M.; Cammi, R.; Mennucci, B.; Pomelli, C.; Adamo, C.; Clifford, S.; Ochterski, J.; Petersson, G. A.; Ayala, P. Y.; Cui, Q.; Morokuma, K.; Malick, D. K.; Rabuck, A. D.; Raghavachari, K.; Foresman, J. B.; Cioslowski, J.; Ortiz, J. V.; Stefanov, B. B.; Liu, G.; Liashenko, A.; Piskorz, P.; Komaromi, I.; Gomperts, R.; Martin, R. L.; Fox, D. J.; Keith, T.; Al-Laham, M. A.; Peng, C. Y.; Nanayakkara, A.; Gonzalez, C.; Challacombe, M.; Gill, P. M. W.; Johnson, B. G.; Chen, W.; Wong, M. W.; Andres, J. L.; Head-Gordon, M.; Replogle, E. S.; Pople, J. A. *Gaussian 98*, revision A.7; Gaussian, Inc.: Pittsburgh, PA, 1998.
(56) Scott, A.; Radom, L. *J. Phys. Chem.* **1996**, *100*, 16502.
(57) Siebrand, W. *J. Chem. Phys.* **1966**, *44*, 4055.
(58) Englman, R.; Jortner, J. *Mol. Phys.* **1970**, *18*, 145.
(59) Myers, A. B.; Pranata, K. S. *J. Phys. Chem.* **1989**, *93*, 5079.